β-decay spectroscopy of the proton drip-line nucleus ^{22}Al

C. G. Wu,[1,*] H. Y. Wu,[1,*] J. G. Li,[1] D. W. Luo,[1] Z. H. Li,[1,†] H. Hua,[1,‡] X. X. Xu,[2,3,§] C. J. Lin,[2,4,‖] J. Lee,[3] L. J. Sun,[2,5] P. F. Liang,[3] C. X. Yuan,[6] Y. Y. Yang,[7] J. S. Wang,[7,8] D. X. Wang,[2] F. F. Duan,[9,7] Y. H. Lam,[7] P. Ma,[7] Z. H. Gao,[7,9] Q. Hu,[7] Z. Bai,[7] J. B. Ma,[7] J. G. Wang,[7] F. P. Zhong,[4,2] Y. Jiang,[1] Y. Liu,[1] D. S. Hou,[7,10] R. Li,[7,10] N. R. Ma,[2] W. H. Ma,[7,11] G. Z. Shi,[7] G. M. Yu,[7] D. Patel,[7] S. Y. Jin,[7,10] Y. F. Wang,[12,7] Y. C. Yu,[12,7] Q. W. Zhou,[13,7] P. Wang,[13,7] L. Y. Hu,[14] S. Q. Fan,[1] X. Wang,[1] H. L. Zang,[1] P. J. Li,[3] Q. Q. Zhao,[3] L. Yang,[2] P. W. Wen,[2] F. Yang,[2] H. M. Jia,[2] G. L. Zhang,[15] M. Pan,[15,2] X. Y. Wang,[15] H. H. Sun,[2] Z. G. Hu,[7] M. L. Liu,[7] R. F. Chen,[7] W. Q. Yang,[7] S. Q. Hou,[7] J. J. He,[16,10] Y. M. Zhao,[5] F. R. Xu,[1] and H. Q. Zhang[2]

(RIBLL Collaboration)

[1]*State Key Laboratory of Nuclear Physics and Technology, School of Physics, Peking University, Beijing 100871, China*

[2]*Department of Nuclear Physics, China Institute of Atomic Energy, Beijing 102413, China*

[3]*Department of Physics, The University of Hong Kong, Hong Kong, China*

[4]*College of Physics and Technology, Guangxi Normal University, Guilin 541004, China*

[5]*School of Physics and Astronomy, Shanghai Jiao Tong University, Shanghai 200240, China*

[6]*Sino-French Institute of Nuclear Engineering and Technology, Sun Yat-Sen University, Zhuhai 519082, China*

[7]*Institute of Modern Physics, Chinese Academy of Sciences, Lanzhou 730000, China*

[8]*School of Science, Huzhou University, Huzhou 313000, China*

[9]*School of Nuclear Science and Technology, Lanzhou University, Lanzhou 730000, China*

[10]*University of Chinese Academy of Sciences, Beijing 100049, China*

[11]*Institute of Modern Physics, Fudan University, Shanghai 200433, China*

[12]*School of Physics and Astronomy, Yunnan University, Kunming 650091, China*

[13]*School of Physical Science and Technology, Southwest University, Chongqing 400044, China*

[14]*Fundamental Science on Nuclear Safety and Simulation Technology Laboratory, Harbin Engineering University, Harbin 150001, China*

[15]*School of Physics, Beihang University, Beijing 100191, China*

[16]*College of Nuclear Science and Technology, Beijing Normal University, Beijing 100875, China*

(Received 9 May 2021; accepted 29 September 2021; published 11 October 2021)

A detailed β-decay spectroscopic study of ^{22}Al was performed at the Radioactive Ion Beam Line in Lanzhou. With the β-γ-particle coincidence measurement by a high-resolution DSSD particle detection array and a high efficiency γ-ray detection array, total eight excited states in ^{22}Mg fed by Gamow-Teller transitions was newly identified. The one-proton, two-proton, and α decays of the IAS at 14046(5) keV in ^{22}Mg, which were partly observed in different experiments before, were identified simultaneously in the present work, providing accurate spectroscopic information about its decay. A more complete β-decay scheme of ^{22}Al was constructed and compared to the shell-model calculations with the USD-type Hamiltonians, USDC and USDB.

DOI: 10.1103/PhysRevC.104.044311

I. INTRODUCTION

The β decays of nuclei close to the drip-line are characterized by the large β-decay energy and small particle separation energy in daughter nuclei, which open up a variety of decay modes [1,2]. One of the interesting decay modes in the proton-rich side is the superallowed β decay to the isobaric analog state (IAS), which is usually located at large excitation energy and followed by multiparticle decay. Because the particle decays of the IAS are all isospin forbidden, the observation of particle emission from the IAS reveals the effect of isospin-symmetry breaking. Therefore, complicated β-decay processes of proton-rich nuclei shed light not only on the structure of the daughter and parent nuclei, but also on the fundamental subatomic symmetries.

To identify the complex decay scheme and to provide a stringent test of the theoretical models, high-resolution experiments are necessary. Owing to recent developments in producing intense rare isotope beams worldwide, as well as efficient particle and γ-ray coincidence detection systems, it has become realizable to measure simultaneously a number of particle branching ratios in one β-decay experiment. In this

*These authors contributed equally to this work.
†zhli@pku.edu.cn
‡hhua@pku.edu.cn
§xinxing@impcas.ac.cn
‖cjlin@ciae.ac.cn

paper, we report a β-decay study of ^{22}Al using β-γ-particle coincidence method.

As the most proton-rich bound Aluminum isotope, the β decay of ^{22}Al is of great interests. Because the β-decay energy of ^{22}Al is 18.60 MeV, well above the one-proton threshold at $S_p = 5504.1$ keV, the two-proton threshold at $S_{2p} = 7936.0$ keV, and α threshold at $S_\alpha = 8142.5$ keV [3]; ^{22}Al is an ideal case for investigation on the β-delayed p, 2p, and α emission. As the first experimentally confirmed β2p emitter, the β2p and βp of ^{22}Al have been studied nearly forty years ago by Cable *et al*. [4,5] using a helium-jet technique. In their experiments, two β2p branches to the ground state and the first excited state in ^{20}Ne, as well as two βp branches to the ground and first excited state in ^{21}Na, were identified. These decay branches were found to proceed via the IAS in ^{22}Mg, which is fed by a superallowed β-decay of ^{22}Al. Consequently, the excitation energy of the T = 2 IAS in ^{22}Mg was determined and the ground state of ^{22}Al was suggested to have a spin-parity 4^+ based on the T = 2 isospin multiplet. Detailed studies of the β2p of ^{22}Al indicated that the dominant two proton emission mechanism is a sequential process [6,7].

In another study of ^{22}Al β decay by Blank *et al*. [8,9] via implanting the ^{22}Al into a silicon detector and into a microstrip gas counter (MSGC), the $\beta\alpha$ branch to the first excited state in ^{18}Ne through the IAS in ^{22}Mg was identified based on the drift-time analysis of emitted particle in the MSGC [10]. The absolute branching ratios for $\beta\alpha$, βp, and β2p have also been determined in this experiment, while the 3^+ rather than 4^+ was suggested for the ground state of ^{22}Al [8,9]. It should be noted that these experiments [4,5,8,9] focus on the measurement of emitted light charged particles, no γ-ray detector was used.

In a recent experiment by Achouri *et al*., in order to establish a more complete decay scheme for ^{22}Al, the β-γ-particle coincidence measurement was used [11]. The ^{22}Al were produced by the fragmentation of ^{36}Ar primary beam and implanted in a stack of three unsegmented silicon detectors, which were also served as β-particle and light charge-particle detectors. The β-delayed γ rays were detected by an EXOGAM germanium clover detector. With the β-γ-particle coincidence measurement, a total of 25 β-delayed particle emissions with absolute branching ratios were identified in this experiment. The spin-parity of ground state in ^{22}Al was assigned to be most likely 4^+ based on a comparison of the experimental results with theoretical calculations and the mirror nucleus [11].

Although significant progress has been made on the experimental study of ^{22}Al β decay, more β-decay experimental measurements of spectroscopy are very desirable. For example, in Ref. [11], three unsegmented silicon detectors were used to measure the emitted particles. With the progress in experimental technology in recent years, the double-sided Si strip detector (DSSD) has been successfully applied to the β-decay studies for the nuclei far from the β-stability line [12–14]. By correlating the implantated nuclei with their subsequent β decays within the same pixel or adjacent pixels of the DSSD, the backgrounds of β-delayed charged particles spectrum will be significantly suppressed. Furthermore, compared to the large unsegmented silicon detector, the small pixel of DSSD has a better resolution for the charged particles. These characters are good for the precise identification of the small particle branching decay path, which is sensitive to particular nuclear structure properties. In addition, as mentioned in Ref. [11], the energy range of γ is limited to 3800 keV, which limits the observation of high-energy γ ray.

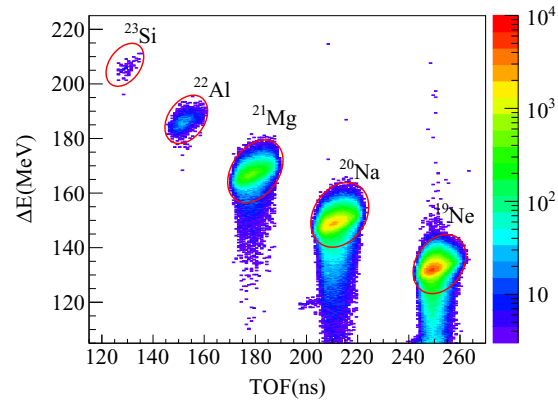

FIG. 1. Particle identification plot for incoming radioactive ions at RIBLL.

In the present paper, we have made a further β-decay spectroscopic study of ^{22}Al using an improved detector configuration, which combines a high-resolution DSSD particle detection array and a high efficiency γ-ray detection array with a broader energy range. With the use of the new detector setup, a more complete experimental decay scheme has been obtained and compared to the shell-model calculations.

II. EXPERIMENT

The experiment was performed at the Heavy Ion Reaction Facility in Lanzhou (HIRFL) [15], China. ^{22}Al was produced by the projectile fragmentation of a 75.6 MeV/nucleon ^{28}Si primary beam on the ^{9}Be target, then it was identified by the Radioactive Ion Beam Line in Lanzhou (RIBLL1) [16] with the combination of energy loss (ΔE), time-of-flight (TOF), and magnetic rigidity ($B\rho$) on an event-by-event basis. As shown in the ΔE-TOF plot in Fig. 1, the radioactive ions are well identified and separated. The average intensity and purity of ^{22}Al in the secondary beam delivered to the detection chamber were 0.79 particles per second (pps) and 0.24%, respectively.

Passing through a stack of aluminum degraders, the radioactive ions were finally implanted in a DSSD array [17–19]. This DSSD detection array was composed of three DSSDs with different thickness (DSSD1 of 142 μm, DSSD2 of 40 μm, and DSSD3 of 304 μm). The subsequent decays were measured by this DSSD detection array and correlated to the preceding implantations by using the position and time information. At the downstream of the DSSD array, three quadrant silicon detectors with thicknesses of 1546 μm, 300 μm, and 300 μm were used to detect the β particles in the decay and were also used as a veto detector for the penetrating light particles along with the beam.

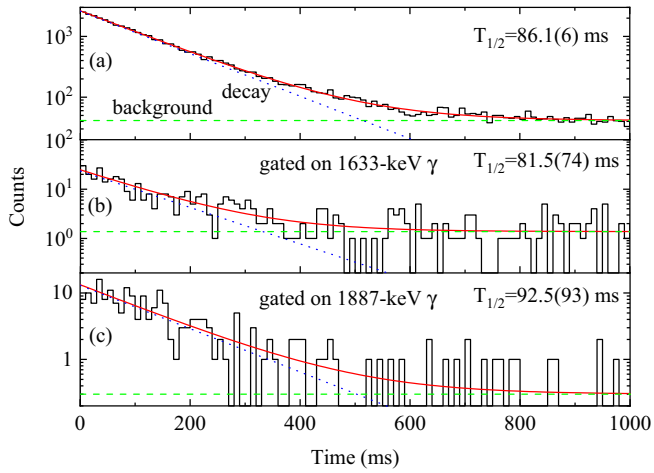

FIG. 2. Decay-time spectrum in coincidence with (a) all the subsequent decay products, (b) 1633-keV γ ray, and (c) 1887-keV γ ray.

The γ rays emitted from β decay of ^{22}Al were measured by a γ-detection array, which consisted of five clover-type high-purity germanium (HPGe) detectors and was placed around the DSSD array. The detection efficiency for 1 MeV γ rays is 4.5(4)%. The experiment was performed in the continuous beam mode. Detailed description of the detector setup and experimental details can be found in Ref. [17].

In the present experiment, the β-delayed proton peaks from ^{25}Si decay with known energies and the corresponding absolute intensities [20] were employed for the proton efficiency calibration, while the well-known β-γ transitions of ^{25}Si [20] and ^{20}Na [21] were used for the β absolute efficiency calibrations. The γ efficiency was determined from the ^{152}Eu standard source and the γ rays following the β-delayed proton emission from ^{22}Al, ^{25}Si, and ^{21}Mg.

III. RESULTS AND DISCUSSION

The β-decay curve of ^{22}Al, obtained by measuring the time difference between the implanted nuclei and all the subsequent decay events in the same pixel of DSSD, was used for the determination of the half-life of ^{22}Al. The results are shown in Fig. 2(a). The decay spectrum was well fitted by an exponential decay component plus a constant background. From the fit, a half-life of 86.1(6) ms was obtained. This value is in good agreement with the previous measured value of 87.3(11) ms with the same continuous beam mode [11], but is slightly smaller than the value of 91.9(14) ms measured in the same experiment using the beam-on/beam-off mode [11].

The energy spectrum of emitted charged-particle in the β decay of ^{22}Al measured by DSSD3 is shown in Fig. 3, where total 29 peaks are identified. The peak energies and their branching ratios are given in Table I and compared with previous measurements [11]. It can be seen that all the peaks observed in the previous experiment except for one weakest peak at 5808 keV have been confirmed in the present experiment. In Fig. 3, a sign of the peak can be seen at 5808 keV, but it is not very sure. With the higher peak/valley ratio and broader energy range for particle energy spectrum, three peaks at 3800 keV (p_{15}), 7000 keV (p_{25}), and 7225 keV (p_{26}) are newly observed. In addition, two higher energy peaks at 8205 keV (p_{28}) and 8516 keV (p_{29}), which were identified in Ref. [8] but not in Ref. [11], are also observed in the present

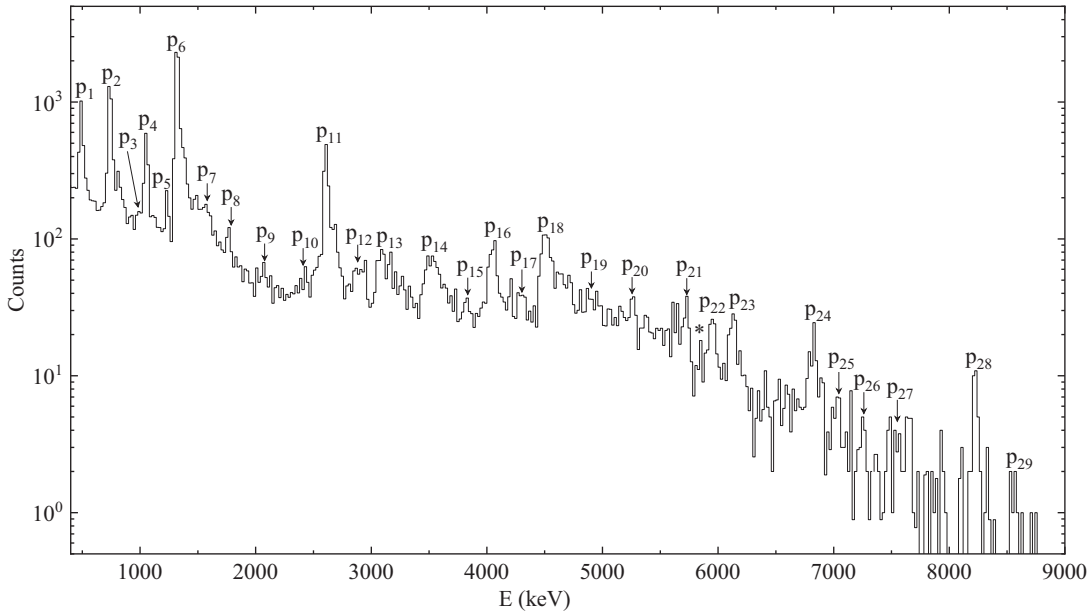

FIG. 3. The energy spectrum of emitted charged-particle in the β decay of ^{22}Al measured by DSSD3. Each particle peak from the β-delayed particle decay of ^{22}Al is labeled with a letter p followed by a number. The proton peak at 5808 keV reported in Ref. [11] (labeled with * at corresponding position) was not observed in present work.

TABLE I. The obtained total decay energies of β-delayed particles and their branching ratios in the present work in comparison with previous results measured by Achouri *et al*. [11]

	This work		Achouri *et al*. [11]	
	Energy (MeV)	Br (%)	Energy (MeV)	Br (%)
p_1	0.470 ± 0.006	4.22 ± 0.12	0.475 ± 0.008	4.73 ± 0.63
p_2	0.717 ± 0.007	7.93 ± 0.17	0.721 ± 0.008	7.39 ± 1.01
p_3	0.970 ± 0.008	0.36 ± 0.06	0.975 ± 0.008	0.25 ± 0.05
p_4	1.033 ± 0.007	2.61 ± 0.10	1.033 ± 0.008	3.00 ± 0.34
p_5	1.213 ± 0.007	0.71 ± 0.07	1.223 ± 0.008	0.75 ± 0.10
p_6	1.299 ± 0.007	19.75 ± 0.26	1.299 ± 0.008	18.51 ± 1.74
p_7	1.525 ± 0.019	3.45 ± 0.14	1.551 ± 0.010	0.81 ± 0.16
p_8	1.743 ± 0.008	0.66 ± 0.07	1.753 ± 0.008	0.45 ± 0.08
p_9	2.029 ± 0.010	0.62 ± 0.07	2.072 ± 0.008	0.48 ± 0.07
p_{10}	2.410 ± 0.030	0.25 ± 0.08	2.503 ± 0.010	0.64 ± 0.13
p_{11}	2.586 ± 0.008	5.55 ± 0.16	2.583 ± 0.008	4.89 ± 0.24
p_{12}	2.870 ± 0.012	0.75 ± 0.08	2.838 ± 0.008	2.11 ± 0.09
p_{13}	3.063 ± 0.009	1.46 ± 0.11	3.088 ± 0.008	1.89 ± 0.07
p_{14}	3.511 ± 0.011	1.57 ± 0.12	3.484 ± 0.008	2.18 ± 0.15
p_{15}	3.800 ± 0.010	0.13 ± 0.06		
p_{16}	4.030 ± 0.010	1.38 ± 0.10 $0.12 \pm 0.01(\alpha)$	4.017 ± 0.008	1.04 ± 0.33 $0.038 \pm 0.017(\alpha)$
p_{17}	4.283 ± 0.012	0.28 ± 0.06	4.224 ± 0.009	0.84 ± 0.11
p_{18}	4.495 ± 0.011	2.36 ± 0.14 $0.72 \pm 0.05(2p)$	4.464 ± 0.008	2.52 ± 0.14 $0.69 \pm 0.08(2p)$
p_{19}	4.864 ± 0.021	0.74 ± 0.09	4.912 ± 0.010	0.27 ± 0.32
p_{20}	5.234 ± 0.013	0.64 ± 0.08	5.177 ± 0.013	0.29 ± 0.11
p_{21}	5.705 ± 0.008	0.58 ± 0.07	5.667 ± 0.008 5.808 ± 0.049	0.35 ± 0.11 0.18 ± 0.55
p_{22}	5.930 ± 0.014	0.46 ± 0.06	5.909 ± 0.056	0.21 ± 0.62
p_{23}	6.106 ± 0.016	0.52 ± 0.05	6.085 ± 0.008	0.41 ± 0.07
p_{24}	6.804 ± 0.019	0.64 ± 0.06	6.774 ± 0.008	0.41 ± 0.12
p_{25}	7.000 ± 0.020	0.18 ± 0.04		
p_{26}	7.225 ± 0.016	0.08 ± 0.02		
p_{27}	7.571 ± 0.070	0.23 ± 0.04	7.517 ± 0.011	0.33 ± 0.07
p_{28}[a]	8.205 ± 0.017	0.16 ± 0.03		
p_{29}[a]	8.516 ± 0.018	0.03 ± 0.01		

[a]Also observed by Blank *et al*. [8].

work. One thing needs to be mentioned that for the peaks 16 and 18, they have contributions not only from βp but also from $\beta\alpha$ and β2p, respectively, which will be discussed in the following with the coincidence relationship analysis.

Figure 4 shows the γ-ray spectrum measured by the γ-ray detection array in coincidence with ^{22}Al β-decay signals in the DSSD particle detection array. Total 12 γ-ray peaks (including 511 keV γ ray) can be clearly seen. Four of them (332-, 1384-, 1113-, and 2497-keV transitions) correspond to the deexcitation from the low-lying excited states in ^{21}Na being fed via βp decay of ^{22}Al, while five of them (1246-, 1986-, 2062-, 2145-, and 4207-keV transitions) come from the $\beta\gamma$ decay of ^{22}Al. The other two transitions at 1633 keV and 1887 keV correspond to the deexcitation of the first excited 2^+ state in ^{20}Ne (β2p decay of ^{22}Al) and ^{18}Ne ($\beta\alpha$ decay of ^{22}Al), respectively.

Figures 2(b) and 2(c) show the β-decay spectrum gated on the 1633- and 1887-keV γ rays, respectively. The half-lives determined from the fitting are 81.5(74) and 92.5(93) ms, respectively, which are consistent with the result obtained from fitting the β-decay spectrum in Fig. 2(a) and further

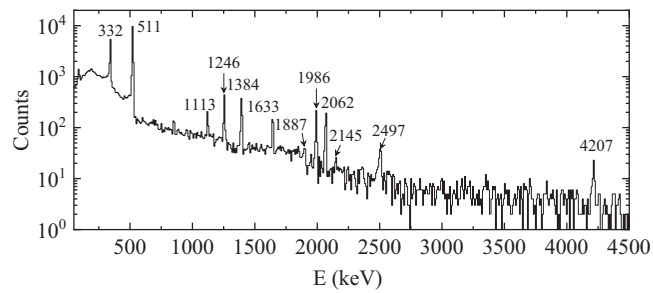

FIG. 4. Energy spectrum of γ rays measured by the γ-ray detection array in coincidence with ^{22}Al β-decay signals in the DSSD particle detection array.

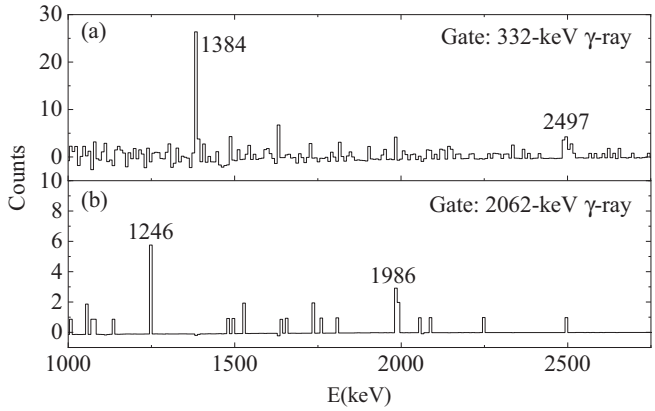

FIG. 5. Coincident γ-ray spectra gated on the (a) 332-keV γ ray and (b) 2062-keV γ ray.

support their origination: from β decay of ^{22}Al. Although the 2497-keV transition in ^{21}Na and 4207-keV transition in ^{22}Mg have been found in many other experiments [22,23], they are firstly observed in the β decay of ^{22}Al due to the combination of a high detection efficiency and a broad energy range for γ rays in the present work. In addition, the γ-ray detection array used in the present work allows us to establish the γ-γ coincidences, which is helpful to unambiguously determine the complex decay scheme. Figures 5(a) and 5(b) present examples of γ coincidence spectra in ^{21}Na and ^{22}Mg, respectively.

Figure 6(a) shows the charged-particle spectrum with coincidence gating condition on the 332-keV γ ray in ^{21}Na, in comparison with raw charged-particle spectrum without any coincidence with the γ rays. For the convenience of comparison, the raw charged-particle spectrum was scaled to match the amplitude of the strongest peak p_6. It can be seen that total 14 proton peaks p_1, p_3, p_4, p_5, p_6, p_7, p_8, p_9, p_{11}, p_{12}, p_{13}, p_{14}, p_{16}, and p_{18} are almost unaffected by the gating condition and in coincidence with the 332-keV γ ray. It should be mentioned that since peaks p_{18} and p_{16} in raw charged-particle spectrum also have contributions from β2p and $\beta\alpha$ branches of ^{22}Al, respectively, they are wider than the corresponding peaks in the coincidence spectrum as shown in Fig. 6(a).

Figures 6(b) and 6(c) show the charged-particle spectrum with coincidence gating condition on the 1384-keV and 1113-keV γ rays in ^{21}Na, respectively. Three proton peaks p_3, p_5, and p_7 are found to be in coincidence with the 1384-keV γ ray, while the p_3 and p_7 are also in coincidence with the 1113-keV γ ray. Base on the γ-particle coincidences, two new states at 9303 and 9864 keV in ^{22}Mg are identified and decay to the excited state at 8333 keV in ^{21}Na. The coincidence relationship and energy summation also indicate that the new 9864-keV state in ^{22}Mg will also directly decay to the excited state at 5836 keV in ^{21}Na via emitting proton p_{16}. Meanwhile, energy summation suggests that the new 9303-keV state in ^{22}Mg will also directly decay to the ground state in ^{21}Na via emitting proton p_{15}.

In Ref. [11], based on the coincidence between the 332-keV γ ray and the 2583-keV proton (p_{11} in the present paper), the state at 8428 keV in ^{22}Mg was identified. Here, with the observation of the coincidence between the 1384-keV γ ray and the 1213-keV proton (p_5) shown in Fig. 6(b), one more new branch from this state to the excited state at 7220 keV in ^{21}Na has been found. In addition, the coincidences between 332-keV γ-ray and proton peaks p_1, p_4, p_6, and p_{11} have been observed in Ref. [11]. Here, with the newly observed coincidences between 332-keV γ-ray and proton peaks p_8, p_9, p_{12}, p_{13}, p_{14}, and p_{18}, six states at 7579, 7865, 8706, 8899, 9347, 10331 keV are firstly identified, respectively. As shown in Fig. 6(a), with coincidence gating condition on the 332-keV γ ray in ^{22}Mg, the proton peak at 717 keV (p_2) was significantly depressed compared to the raw charged-particle spectrum. Hence, such pattern unambiguously indicates that p_2 comes from the proton decay to the ground state of ^{21}Na. For the higher energy protons (>5000 keV), only proton peak p_{21} is found to be in coincidence with the 332-keV γ rays in ^{21}Na [not shown in Fig. 6(a)]. Based on the energy summation consideration, the proton peaks p_{21}, p_{24}, p_{28}, and p_{29} correspond to the proton decay from IAS in ^{22}Mg to the excited states and ground state in ^{21}Na, respectively, which were also suggested in Refs. [4,8,11].

For the β2p and $\beta\alpha$ branches of ^{22}Al, Figs. 6(d) and 6(e) show the charged-particle spectrum with coincidence gating condition on the 1633-keV γ ray ($2_1^+ \rightarrow 0^+$) in ^{20}Ne and 1887-keV γ rays ($2_1^+ \rightarrow 0^+$) in ^{18}Ne, respectively. The peaks p_{18} and p_{16} are clearly seen in the coincidence spectra, and correspond to decaying from IAS in ^{22}Mg to excited states in ^{20}Ne and ^{18}Ne, respectively, which are consistent with the previous measurement by Achouri *et al*. [11]. Meanwhile, the peak p_{23} can be ascribed to decaying to ground state in ^{20}Ne based on the energy summation.

Based on the β-γ-particle coincidence analysis and comparison with the theoretical results discussed in the following, a new decay scheme of ^{22}Al is constructed and shown in Fig. 7. After correction for the proton, β, and γ detection efficiencies, and normalization to the total number of ^{22}Al implanted, the absolute branching ratios to different states are presented. The summed branching ratios are 91.6(51)%. The unassigned transitions such as p_{10}, p_{17}, p_{19}, p_{20}, p_{22}, p_{25}, p_{26}, and p_{27}, as well as the unobserved weak proton groups, will contribute to the missing branching ratios.

Compared to the previous β-decay experiments [4,5,8,9,11], total eight excited states in ^{22}Mg fed by Gamow-Teller transitions are newly identified in the present paper. Base on the newly observed coincidences between γ-rays and proton peaks, these new states in ^{22}Mg decay to the excited state in ^{21}Na. In Ref. [11], the levels at 6306 and 6869 keV in ^{22}Mg were assigned to 4^+ and 3^+, respectively. Here, the theoretical results shown in Fig. 8 indicate that the spin-parities of these two levels are most likely 3^+ and 4^+, respectively.

The gross features of decay of IAS in ^{22}Mg are consistent with previous results. Only the branching ratio of 0.12(1)% for the α decay of IAS is smaller than the value of 0.31(9)% obtained in Refs. [8,9], and larger than the value of 0.038(17)% obtained in Ref. [11]. In addition, eight proton peaks (p_{10}, p_{17}, p_{19}, p_{20}, p_{22}, p_{25}, p_{26}, p_{27}) are found not in coincidence with any γ rays in ^{21}Na, ^{20}Ne, and ^{18}Ne. They also can not be ascribed to the transitions from a established state to the

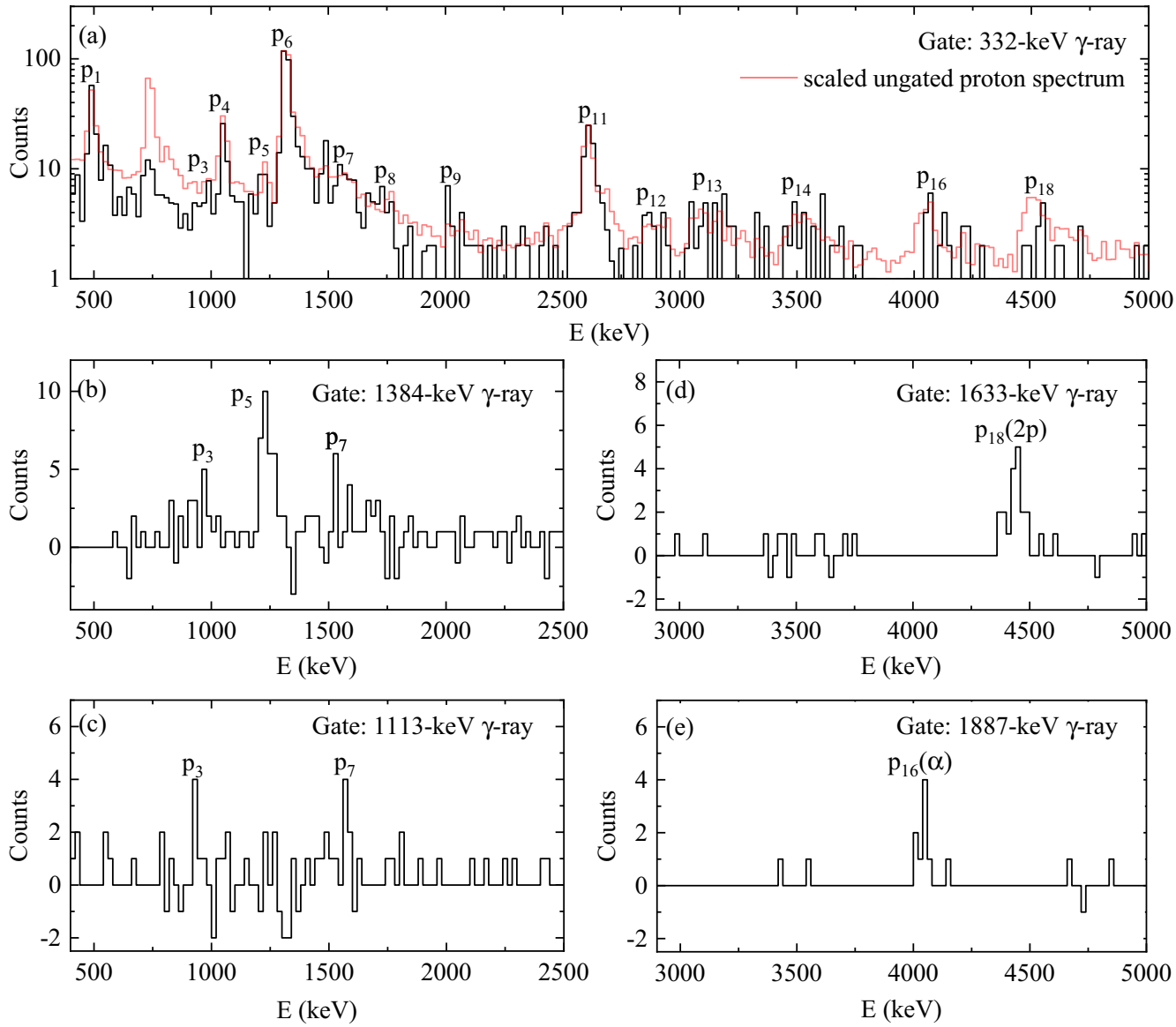

FIG. 6. The energy spectra of emitted charged-particle in coincidence with the (a) 332-keV γ ray, (b) 1384-keV γ ray, (c) 1113-keV γ ray, (d) 1633-keV γ ray, and (e) 1887-keV γ ray. For the convenience of comparison, the raw charged-particle spectrum was scaled to match the amplitude of the strongest peak p_6 and plotted in Fig. 6(a) with red line.

ground state in above nuclei based on the energy summation. These proton peaks most likely correspond to the one-proton decays from excited states in ^{22}Mg to the ground state in ^{21}Na. Firm determination of their positions in the decay scheme needs more experimental work.

To further investigate the β decay of ^{22}Al, shell-model calculations have been performed using the KSHELL code [24] in the *sd*-shell model space with the state-of the-art isospin nonconserving interaction USDC developed by Mahilligan and Brown [25], as well as the isospin conserving interaction USDB [26]. In the present shell-model calculations, a quenching factor of 0.76 is included [27]. They predicted a half-life of 95.3 and 92.0 ms for the β decay of ^{22}Al with USDC and USDB interactions, respectively, which are slightly larger than the 86.1(6) ms measured here. The calculated levels with branching ratios in ^{22}Mg are plotted in Fig. 8 in comparison with the experimental results. It can be seen that both the USDC and USDB calculations give an overall satisfactory description of experimental data, particularly for the low-lying levels, which makes the correspondence between the experimental results and calculations possible. At high excitation energy region, the high density of levels makes such correspondence difficulty. Only for the level at 8.429 MeV with a branching ratio of 6.26%, since USDC and USDB calculations predict a 5^+ level at 8.456 MeV with a branching ratio of 5.53% and 5^+ level at 8.598 MeV with a branching ratio of 5.62%, respectively, it can be tentatively assigned to a spin-parity 5^+.

According to the USDC and USDB calculations, the energies of the IAS in ^{22}Mg are 13.854 and 13.892 MeV,

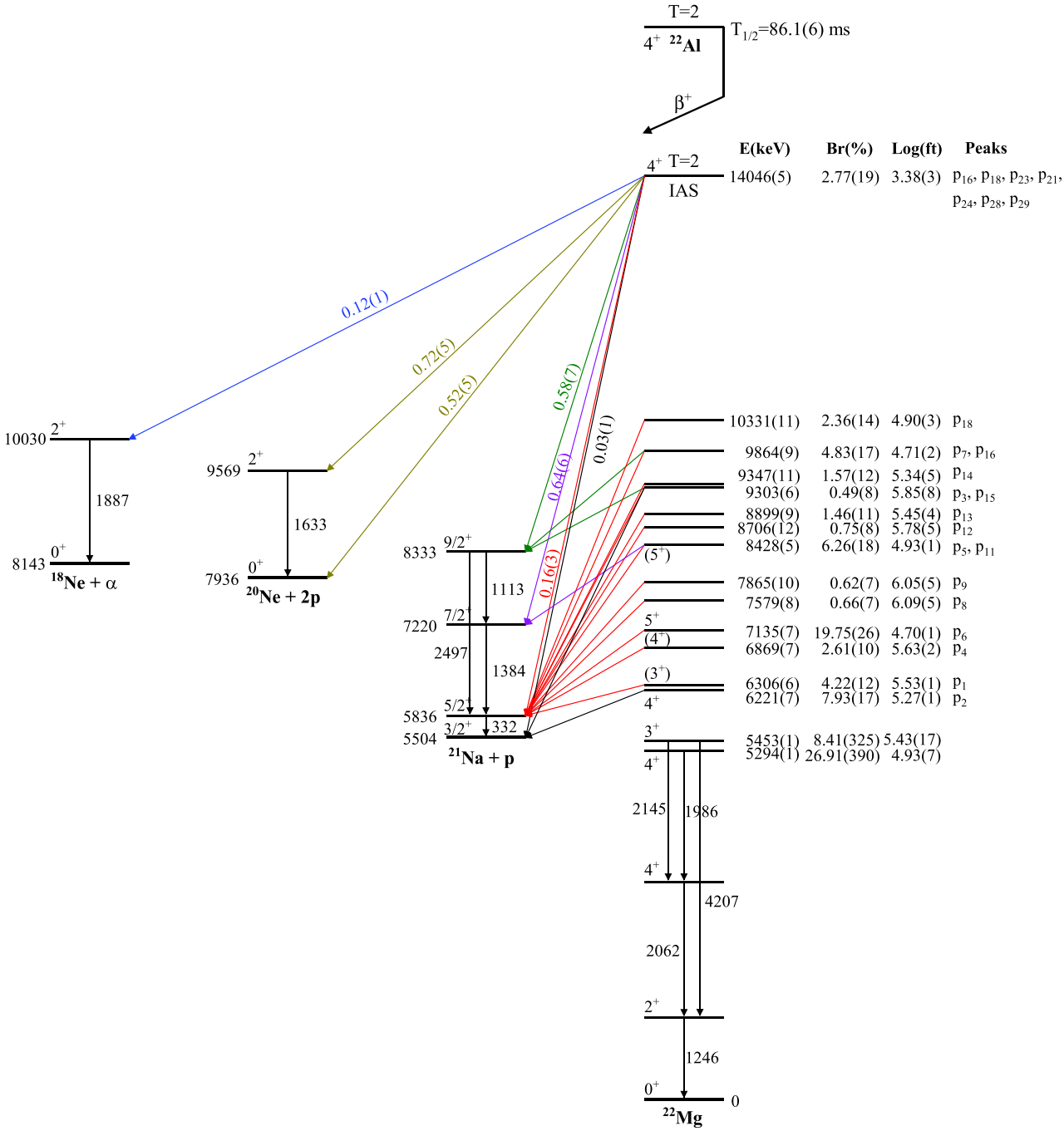

FIG. 7. Decay scheme for ^{22}Al. All the energies and intensities labeled in the scheme are deduced from the present work. The energies of the ground states of ^{18}Na, ^{20}Ne, and ^{21}Na are labeled by the separation energies of α, two-proton, and one-proton, respectively [3]. The peak labels represent that the peaks in Fig. 3 are emitted from corresponding energy levels.

respectively, which are in reasonable agreement with the experimental energy 14.046(5) MeV. Its isospin forbidden decay paths to the low-lying states of ^{21}Na, ^{20}Ne, and ^{18}Ne have been calculated with different isospin nonconserving interactions [8,11,28,29]. The predicted decay pattern of the IAS in different calculations are very similar and are in overall consistent with the present experimental results. For the one-proton decay of IAS, both theoretical [28,29] and experimental results indicate the strongest path is to the $\frac{7}{2}^+$ state at 1716 keV in ^{21}Na, while for the two-proton decay of IAS, the branching ratio obtained by theoretical calculations assuming a sequential two-proton emission [8,11] is in reasonable agreement with experimental data. In addition, according to calculations by Brown [28], the branching ratio for direct

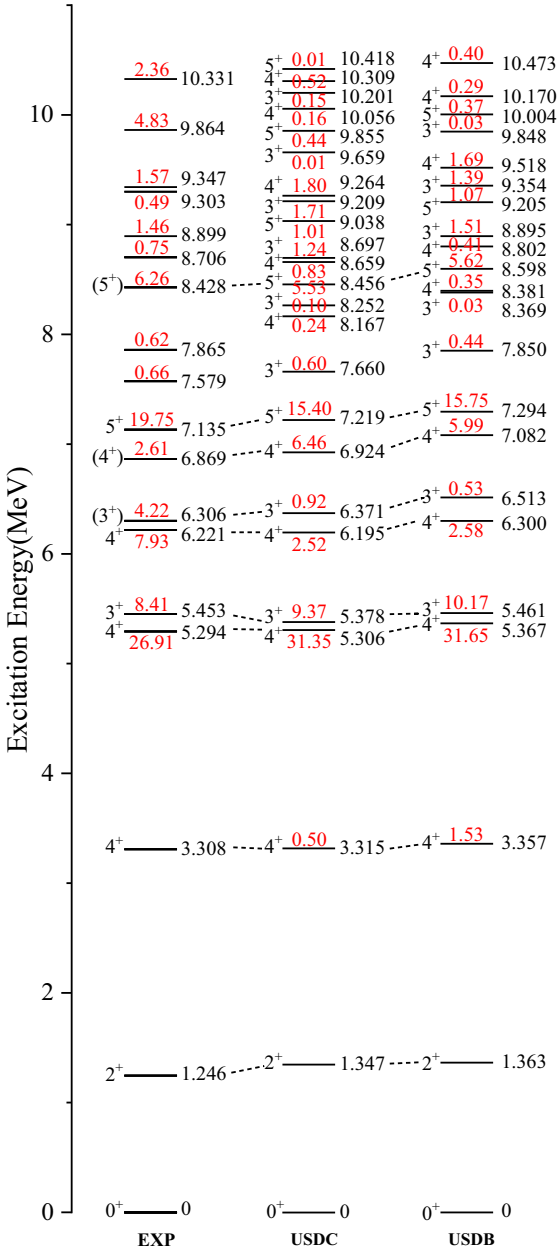

FIG. 8. Comparison of the calculated levels with branching ratios with the experimental results of ^{22}Al β decay measured in the present work. The theoretical and experimental branching ratios are labeled with red color.

two-proton (^{2}He) emission from the IAS in ^{22}Mg to the first excited state in ^{20}Ne is noteworthy. In a recent experiment [30], the probability of ^{2}He emission from the IAS of ^{22}Mg to the first excited state of ^{20}Ne was found to be 29(13)%. Only for the α decay of IAS to the first excited state in ^{18}Ne, the experimental branching ratio of 0.12(1)% is larger than the theoretical value of 0.02% in Ref. [28].

IV. CONCLUSIONS

A detailed study of the β decay of ^{22}Al was performed at RIBLL1. The ^{22}Al was produced by the projectile fragmentation of a 75.6 MeV/nucleon ^{28}Si primary beam on the ^{9}Be target. With a continuous-beam method, a high-resolution DSSD particle detection array and a high efficiency γ-ray detection array with a broad energy range were used. Based on the β-γ-particle coincidence measurement, total eight excited states in ^{22}Mg fed by Gamow-Teller transitions were identified. The one-proton, two-proton, and α decays of the IAS at 14046 keV in ^{22}Mg, which were partly observed in previous experiments, were measured simultaneously in the present work, providing accurate spectroscopic information about its decay. A more complete β-decay scheme of ^{22}Al was constructed. Shell-model calculations provide a good description of decay properties for ^{22}Al. Total eight proton branches observed in the present work cannot be firmly determined their positions in the decay scheme of ^{22}Al. Hence, more experimental works are highly desirable.

ACKNOWLEDGMENTS

We would like to acknowledge the staff of HIRFL for providing the ^{28}Si primary beam and the staff of RIBLL1 for all kinds of assistance. This work is support by the National Key Research and Development Program of China under Grants No. 2018YFA0404403, No. 2018YFA0404404, and No. 2016YFA0400503, the National Natural Science Foundation of China under Grants No. 11775003, No. 12035001, No. 12075006, No. 11675003, No. 12022501, No. U1932206, No. U1632136, No. 11635015, No. 11805120, No. 11775316, and No. U1867212, the Strategic Priority Research Program of the Chinese Academy of Sciences, Grant No. XDB34010300, the Continuous Basic Scientific Research Project No. WDJC-2019-13, and the Leading Innovation Project under Grants No. LC192209000701 and No. LC202309000201.

[1] B. Blank and M. J. G. Borge, Prog. Part. Nucl. Phys. **60**, 403 (2008).
[2] M. Pfützner, M. Karny, L. V. Grigorenko, and K. Riisager, Rev. Mod. Phys. **84**, 567 (2012).
[3] M. Wang, W. J. Huang, F. G. Kondev, G. Audi, and S. Naimi, Chin. Phys. C **45**, 030003 (2021).
[4] M. D. Cable, J. Honkanen, R. F. Parry, H. M. Thierens, J. M. Wouters, Z. Y. Zhou, and J. Cerny, Phys. Rev. C **26**, 1778 (1982).
[5] M. D. Cable, J. Honkanen, R. F. Parry, S. H. Zhou, Z. Y. Zhou, and J. Cerny, Phys. Rev. Lett. **50**, 404 (1983).
[6] M. D. Cable, J. Honkanen, E. C. Schloemer, M. Ahmed, J. E. Reiff, Z. Y. Zhou, and J. Cerny, Phys. Rev. C **30**, 1276 (1984).
[7] R. Jahn, R. L. McGrath, D. M. Moltz, J. E. Reiff, X. J. Xu, J. Aysto, and J. Cerny, Phys. Rev. C **31**, 1576 (1985).
[8] B. Blank, F. Boué, S. Andriamonje, S. Czajkowski, R. D. Moral, J. P. Dufour, A. Fleury, P. Pourre, M. S. Pravikoff, N. A. Orr, K. H. Schmidt, and E. Hanelt, Nucl. Phys. A **615**, 52 (1997).

[9] S. Czajkowski, S. Andriamonje, B. Blank, F. Boué, R. Del Moral, J. P. Dufour, A. Fleury, E. Hanelt, N. A. Orr, P. Pourre, M. S. Pravikoff, and K. H. Schmidt, Nucl. Phys. A **616**, 278 (1997).

[10] B. Blank, C. Marchand, R. D. Moral, J. P. Dufour, L. Faux, A. Fleury, and M. S. Pravikoff, Nucl. Instrum. Methods Phys. Res. A **330**, 83 (1993).

[11] N. L. Achouri, F. de Oliveira Santos, M. Lewitowicz, B. Blank, J. Äystö, G. Canchel, S. Czajkowski, P. Dendooven, A. Emsallem, J. Giovinazzo *et al.*, Eur. Phys. J. A **27**, 287 (2006).

[12] L. J. Sun, X. X. Xu, C. J. Lin, J. S. Wang, D. Q. Fang, Z. H. Li, Y. T. Wang, J. Li, L. Yang, N. R. Ma *et al.*, Nucl. Instrum. Methods Phys. Res. A **804**, 1 (2015).

[13] J. Büscher, J. Ponsaers, R. Raabe, M. Huyse, P. Van Duppen, F. Aksouh, D. Smirnov, H. O. U. Fynbo, S. Hyldegaard, and C. A. Diget, Nucl. Instrum. Methods Phys. Res. B **266**, 4652 (2008).

[14] G. Raciti, G. Cardella, M. De Napoli, E. Rapisarda, F. Amorini, and C. Sfienti, Phys. Rev. Lett. **100**, 192503 (2008).

[15] W. L. Zhan, J. W. Xia, H. W. Zhao, G. Q. Xiao, Y. J. Yuan, H. S. Xu, K. D. Man, P. Yuan, D. Q. Gao, X. T. Yang, M. T. Song, X. H. Cai, X. D. Yang, Z. Y. Sun, W. X. Huang, Z. G. Gan, and B. W. Wei, Nucl. Phys. A **805**, 533c (2008).

[16] Z. Sun, W. L. Zhan, Z. Y. Guo, G. Xiao, and J. X. Li, Nucl. Instrum. Methods Phys. Res. A **503**, 496 (2003).

[17] L. J. Sun, X. X. Xu, C. J. Lin, J. Lee, S. Q. Hou, C. X. Yuan, Z. H. Li, J. José, J. J. He, J. S. Wang, D. X. Wang, H. Y. Wu, P. F. Liang, Y. Y. Yang, Y. H. Lam, P. Ma, F. F. Duan, Z. H. Gao, Q. Hu, Z. Bai *et al.* (RIBLL Collaboration), Phys. Rev. C **99**, 064312 (2019).

[18] P. F. Liang, L. J. Sun, J. Lee, S. Q. Hou, X. X. Xu, C. J. Lin, C. X. Yuan, J. J. He, Z. H. Li, J. S. Wang, D. X. Wang, H. Y. Wu, Y. Y. Yang, Y. H. Lam, P. Ma, F. F. Duan, Z. H. Gao, Q. Hu, Z. Bai, J. B. Ma *et al.* (RIBLL Collaboration), Phys. Rev. C **101**, 024305 (2020).

[19] G. Z. Shi, J. J. Liu, Z. Y. Lin, H. F. Zhu, X. X. Xu, L. J. Sun, P. F. Liang, C. J. Lin, J. Lee, C. X. Yuan, S. M. Wang, Z. H. Li, H. S. Xu, Z. G. Hu, Y. Y. Yang, R. F. Chen, J. S. Wang, D. X. Wang, H. Y. Wu, K. Wang *et al.*, Phys. Rev. C **103**, L061301 (2021).

[20] J. C. Thomas, L. Achouri, J. Aysto, R. Beraud, B. Blank, G. Canchel, S. Czajkowski, P. Dendooven, A. Ensallem, and J. Giovinazzo, Eur. Phys. J. A **21**, 419 (2004).

[21] E. T. H. Clifford, E. Hagberg, J. C. Hardy, H. Schmeing, R. E. Azuma, H. C. Evans, V. T. Koslowsky, U. J. Schrewe, K. S. Sharma, and I. S. Towner, Nucl. Phys. A **493**, 293 (1989).

[22] R. B. Firestone, Nucl. Data Sheets **127**, 1 (2015).

[23] M. S. Basunia, Nucl. Data Sheets **127**, 69 (2015).

[24] N. Shimizu, T. Mizusaki, Y. Utsuno, and Y. Tsunoda, Comput. Phys. Commun. **244**, 372 (2019).

[25] A. Magilligan and B. A. Brown, Phys. Rev. C **101**, 064312 (2020).

[26] B. A. Brown and W. A. Richter, Phys. Rev. C **74**, 034315 (2006).

[27] B. Brown and B. Wildenthal, At. Data Nucl. Data Tables **33**, 347 (1985).

[28] B. A. Brown, Phys. Rev. Lett. **65**, 2753 (1990).

[29] N. Smirnova, Y. H. Lam, and E. Caurier, Acta Phys. Pol., B **44**, 479 (2013).

[30] Y. T. Wang, D. Q. Fang, K. Wang, X. X. Xu, L. J. Sun, P. F. Bao, Z. Bai, X. G. Cao, Z. T. Dai, B. Ding *et al.*, Phys. Lett. B **784**, 12 (2018).